



APPLICATION OF NON-CONTACT MEASUREMENT OF OPTOTRAK-CERTUS IN DYNAMIC MODEL TEST OF AN INTAKE TOWER

C. Jiang⁽¹⁾, HY. Zhang⁽²⁾, LJ. Zhang⁽³⁾, SM. Liu⁽⁴⁾

⁽¹⁾ Master degree candidate, College of water conservancy and hydropower engineering, Hohai University, Nanjing, China, jiangcai@hhu.edu.cn

⁽²⁾ Associate Professor, College of water conservancy and hydropower engineering, Hohai University, Nanjing, China, zhanghanyun@hhu.edu.cn

⁽³⁾ Professor, College of water conservancy and hydropower engineering, Hohai University, Nanjing, China, ljzhang@hhu.edu.cn

⁽⁴⁾ Master degree candidate, College of water conservancy and hydropower engineering, Hohai University, Nanjing, China, 1175232643@qq.com

Abstract

Optotrak-Certus measurement technology uses three high-speed infrared cameras to track the infrared light emitted by the markers, thereby recording the spatial coordinates and rotation information of the markers under different loads. This technology has the advantages of non-destruction, full-dimension, wide measuring volume and simple operation. In this paper, Optotrak-Certus technology was applied in the dynamic model test of a hydraulic intake tower, in order to perform full-time, real-time dynamic measurement of the displacement of key positions of the intake tower model. Based on Savitzky-Golay smoothing method, twelve smoothing modes were designed to digitally filter the obtained displacement data, and the obtained filtering results were subjected to differential processing to obtain an acceleration waveform. By comparing with acceleration data collected by traditional sensors, the optimal smoothing parameter of the displacement data was determined. The results showed that after the displacement data was filtered and differentiated by the optimal smoothing parameter, the obtained acceleration data fits the measured acceleration data fairly well, which indicated the effectiveness and availability of using Optotrak-Certus to obtain acceleration data indirectly.

Key words: shaking table; Intake Tower; Non-contact measurement; Optotrak-Certus; Savitzky-Golay smoother

1. Introduction

The shaking table dynamic model test [1, 2] has been one of the important methods to study the seismic performance of hydraulic structures. The traditional contact measurement technology in the model test is restricted by the measurement principle and equipment working conditions, and has certain restrictions on the number, dimensions and positions of the measurement points. Displacement gages, strain gauges, and acceleration sensors and their connected acquisition data lines must work properly in anhydrous and dry conditions. Hydraulic structural model tests need to be performed under water in order to simulate the real working conditions, especially for intake towers and ship lifts, which are surrounded by water. The waterproof requirement of contact test equipment has always been one of the key technical issues restricting the development of test level.

In recent years, the development of non-contact measurement technologies such as digital image correlation technology (DIC) [3], close-range photogrammetry [4] and Optotrak-Certus [5, 6] has made up for the shortcomings of traditional contact measurement technologies. The non-contact testing techniques are widely applied in the study of materials and structural properties [7, 8].

Optotrak-Certus measurement technology (OC), a high-speed real-time six-dimensional dynamic tracking system, is applied in the hydraulic intake tower model test in order to overcome the difficulties of using contact measurement, for instance, limitation of the number of measuring points, complication of the data lines, and the requirement of the waterproofing. OC technology has the advantages of non-destruction, full-dimension, wide measuring volume and simple operation. It has been widely used in high-speed, high-



frequency multi-point tracking field and dynamic real-time measurement of spatial coordinates and rotation information.

In the dynamic model test of the intake tower, the acceleration amplification effect is one of the main seismic performances to investigate. At present, there are few non-contact measurement technologies that directly obtain acceleration. Collecting displacement and then performing differential calculation is a common method to obtain acceleration. However, in the shaking table model test, the acquisition instrument is affected by noise, and the noise signal in the collected data is relatively large. If the acceleration is directly obtained by second differential of the collected displacement data, the interference signals will be amplified by the differential operation, which will seriously impact on the accuracy of acceleration. Savitzky-Golay smoothing technology [9,10,11] (S-G smoother) is a special low-pass filter based on the least square method that smoothes noise directly in the time domain, and the purpose of de-noising is achieved by determining two smoothing parameters, the degree of polynomial fitting and the number of smoothing points. This method can retain the maximum and minimum values of the data during the smoothing process, and ensure that the characteristics such as the shape of the collected signal do not change.

In this paper, on basis of S-G smoother, the displacement data collected by OC technology was smoothed by selecting different smoothing parameters, and then obtained acceleration data through second-order differential operation. The calculated acceleration data obtained by the differentiation was compared with the measured acceleration data collected by the traditional acceleration sensor, the optimal smoothing parameters of the S-G smoother were determined, and the feasibility of the application of the OC technology in the hydraulic structural dynamic model tests was evaluated.

2. Optotrak-certus measurement technology and data processing

Optotrak-Certus measurement technology uses three high-resolution and high-speed infrared array cameras to track the infrared light emitted by the markers (as shown in Fig. 1), so as to record the spatial coordinates and rotation information of the markers under different loading or different working cases. The collection frequency of this technology is as high as 2000 Hz, and the markers actively emit light. The system automatically recognizes the codes and outputs them in real time, and it can collect the coordinate information of 512 markers at most. Fig. 2 shows the arrangement of OC equipment and the model.

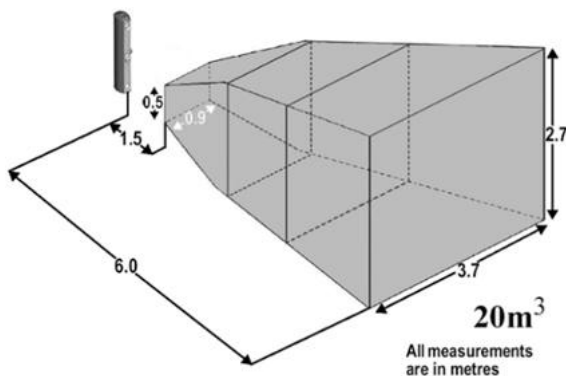


Fig. 1 – OC technology measurement volume



Fig. 2 – The arrangement of OC equipment

Before the start of the shaking table test, the markers are fixed on the model. The infrared light emitted by the diode in the marker is captured by three cameras on the stabilizer bar to determine the initial spatial position (X_0 , Y_0) of the markers. During the test, the OC equipment dynamically captures the infrared light emitted by the markers throughout the entire process, thereby determining the spatial position (X_t , Y_t) of the markers at any time relative to the initial position during the entire excitation period. Suppose that the spatial position of marker 1 at time $t = 0$ before a certain excitation starts is (X_0 , Y_0), and the spatial position at time t during the excitation is (X_t , Y_t), then the displacement of marker 1 during time t is:



$$U_t = X_t - X_0 \quad (1)$$

$$V_t = Y_t - Y_0 \quad (2)$$

Where, U_t is the X-direction displacement of the marker 1 in time 0-t, and V_t is the Y-direction displacement of the marker 1 within 0-t.

3. Savitzky-Golay smoother principle

Savitzky-Golay smoothing technology is a special low-pass time-domain filter. If only the original data is smoothed, the parameters of SG smoothing include the degree of fitting polynomial n and the number of smoothing points of $2m + 1$. In the S-G smoothing process, $2m + 1$ smoothing points are regarded as a window, and all data points in each window are subjected to a local least squares fit to determine the polynomial fitting curve equation of the window. Substituting the abscissa of the center point of the window into the curve equation, the smooth value of the point is obtained. After a window is calculated, slide the data window (that is, delete the leftmost point and increase the rightmost point) to recalculate until the rightmost point is determined. This process achieves smooth processing of all data points.

Suppose a set of data is $y(i)$, $i = -m, \dots, 0, \dots, m$. Use the n th degree polynomial $f(i)$ to fit this set of data, that is:

$$f_i = b_0 + b_1 i + b_2 i^2 + \dots + b_n i^n = \sum_{k=0}^n b_k i^k \quad (3)$$

Where b_i is a polynomial coefficient, According to the principle of least squares, the curve fitting effect is best when the sum of the squared errors ε of the smoothed values of the data points and the measured values is the smallest. Among them,

$$\varepsilon = \sum_{i=-m}^m (f_i - y_i)^2 = \sum_{i=-m}^m (\sum_{k=0}^n b_k i^k - y_i)^2 \quad (4)$$

When the derivative of ε for each coefficient is 0, there is a minimum value, that is:

$$\frac{\partial \varepsilon}{\partial b_r} = 0, \quad (r = 0, 1, 2, \dots, n) \quad (5)$$

Substituting Eq. (4) into Eq. (5), and simplifying it to:

$$\sum_{k=0}^n b_k \sum_{i=-m}^m i^{k+r} = \sum_{i=-m}^m y_i i^r \quad (6)$$

Suppose,

$$F_r = \sum_{i=-m}^m y_i i^r, \quad S_{k+r} = \sum_{i=-m}^m i^{k+r} \quad (7)$$

So,

$$F_r = \sum_{k=0}^n b_k S_{k+r} \quad (8)$$

Given the number of polynomial fittings n , the number of single-sided points m of the smoothing window, and the measured values $y(i)$ of each data point, substituting these into the Eq. (7) and Eq. (8), the polynomial degree b_k ($k=0, 1, \dots, n$) can be obtained, and the fitting equation $f(i)$ can be determined.

4. Analysis scheme

4.1 Cases

In order to compare the validity of the acceleration data (calculated acceleration) obtained indirectly by OC measured displacement with the acceleration data (measured acceleration) obtained by traditional acceleration sensor, the collected data under the excitation of the measured ground motion Landers and artificial acceleration were compared for absolute maximum value and response spectrum curve, respectively. The measured acceleration was filtered to avoid the background noise interference. Table 1 shows the



seismic acceleration parameters in two cases. The stream direction is the X direction, and the cross-stream direction is the Y direction.

4.2 Selection of markers

A total of 7 OC markers were arranged in the test. M2 located on the top of the hoist chamber, M4 located on the top of the lower column of the hoist chamber and the M6 on the top of the main tower were selected. As shown in Fig. 3, the number of acceleration sensors corresponding to the three markers was A2, A4, and A5, respectively. The sampling frequency of the acceleration sensor was 1000 Hz while the sampling frequency of the OC measured displacement was 500 Hz with an accuracy of 0.1mm.

Table 1 – Seismic acceleration parameters

Case	Earthquake Name	Record Duration (s)		PGA(g)	
		Original duration	Test duration	Stream(X)	Cross-stream(Y)
C1	Landers	40	6.325	0.130	0.135
C2	Artificial acceleration	45	7.115	0.1	0.1

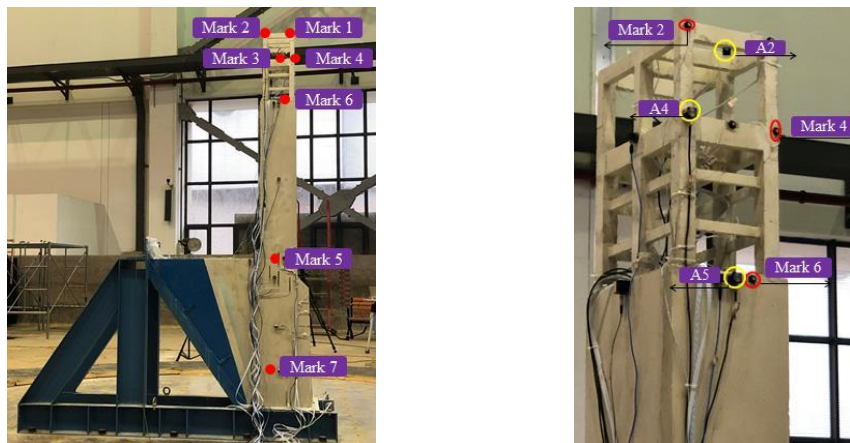


Fig. 3 – The position of the key points

4.3 Analysis scheme

By comparing with multiple sets of data and using a second-order polynomial fit, the characteristics of the processed data can be effectively retained. In order to obtain a smoother calculated acceleration waveform, the smooth points are taken as odd points within 3-25. A total of 12 smoothing modes are used to filter the X and Y displacement data. Under each case, the displacement data collected at the selected three key position markers were subjected to SG smooth filtering, and the calculated acceleration was obtained through a second differential operation. By calculating the relative error of the maximum absolute value of the acceleration and the degree of fit of the response spectrum of acceleration, the degree of agreement between the calculated acceleration and the measured acceleration was evaluated, so as to determine the optimal smoothing parameter from the measured displacement to the calculated acceleration.

5. Results and discussions

5.1 Results of M6

5.1.1 Case 1



Under case 1 excitation, the absolute maximum acceleration in the X-direction and Y-direction collected by the acceleration sensor A5 were 3.7 m/s^2 and 9.42 m/s^2 , respectively. The relative error curve between the maximum measured acceleration and the maximum calculated acceleration obtained indirectly by OC technology is shown in Fig. 4. It is shown that there is a threshold value for the number of smooth points. The closer the threshold value is, the smaller the relative error between the two acceleration values is, and the higher the degree of fit is. Among them, when the number of smoothing points is 3 points, the relative error of maximum acceleration is as high as 117%; when the number of smoothing points is 15 points, the relative error is more than 25%, and the same characteristics are shown in the analysis of other key points in all two cases. Therefore, the data with 5, 7, 9, 11, 13 smooth points are selected to analyze and compare in detail.

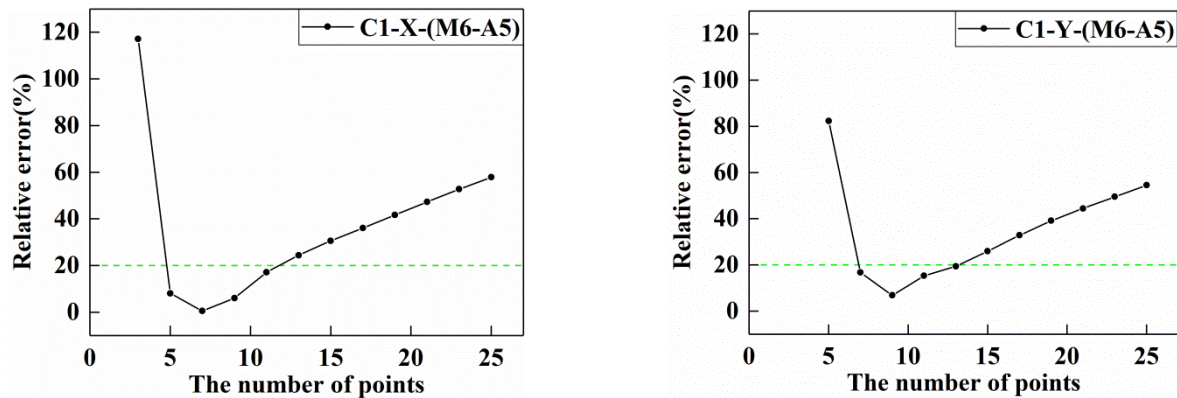


Fig. 4 – Relative error curve of maximum acceleration (C1-M6-A5)

The relative error results of the maximum accelerations in X and Y directions under this case are shown in Table 2. For X-direction acceleration, when the number of smooth points is 5 to 11, the relative error between the two types of maximum acceleration is within 20%. The optimal number of smooth points is 7 points, and the relative error of the maximum value is as low as 0.54%. The time history curves of X-direction displacement directly collected at the M6 and acceleration calculated under the optimal smoothing parameters are shown in Fig. 5. The time history curve of calculated acceleration and the time history curve of measured acceleration fit well, as shown in Fig. 6. In addition, as shown in Fig. 7, the two response spectrum curves of acceleration basically coincide, and the fit between them is good.

Table 2 – C1-The relative error of maximum acceleration (M6-A5)

Direction	The number of points	The maximum measured acceleration (m/s^2)	The maximum calculated acceleration (m/s^2)	Relative error (%)
X	5	3.70	4.00	8.11
	7		3.72	0.54
	9		3.48	5.95
	11		3.07	17.03
	13		2.80	24.32
Y	5	9.42	17.18	82.38
	7		10.99	16.67
	9		8.78	6.79
	11		7.98	15.29
	13		7.59	19.43

For Y-direction acceleration, when the number of smooth points is 7 to 13, the relative error of maximum value is within 20%. The results are shown in Table 2. Among them, the optimal smoothing point



is 9 points, and the relative error between the two kinds of maximum acceleration is 6.79%. Similarly, it can be seen from Fig. 8 that the two response spectrum curves of acceleration is basically coincided, and the fitting degree is fine.

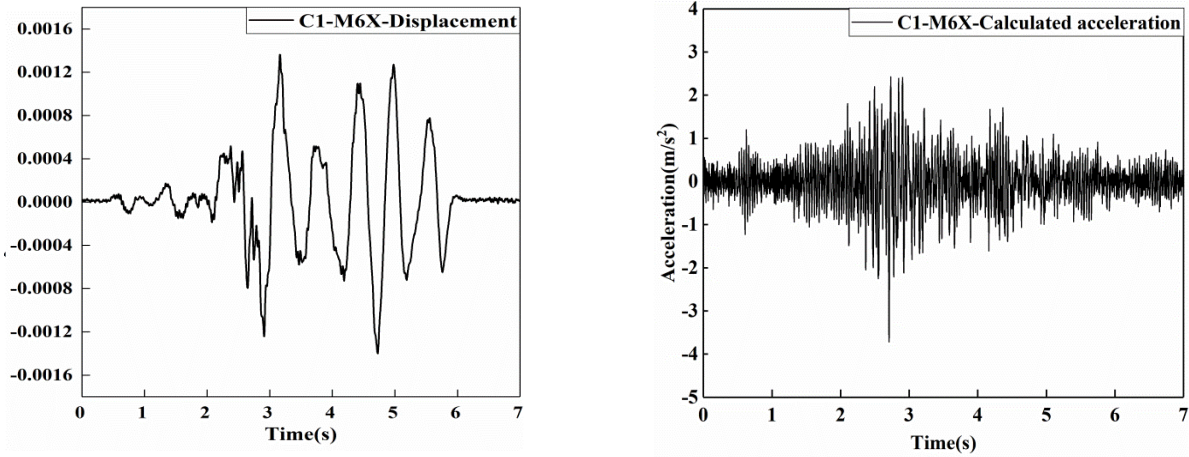


Fig. 5 – Time history of displacement and acceleration (C1-M6X)

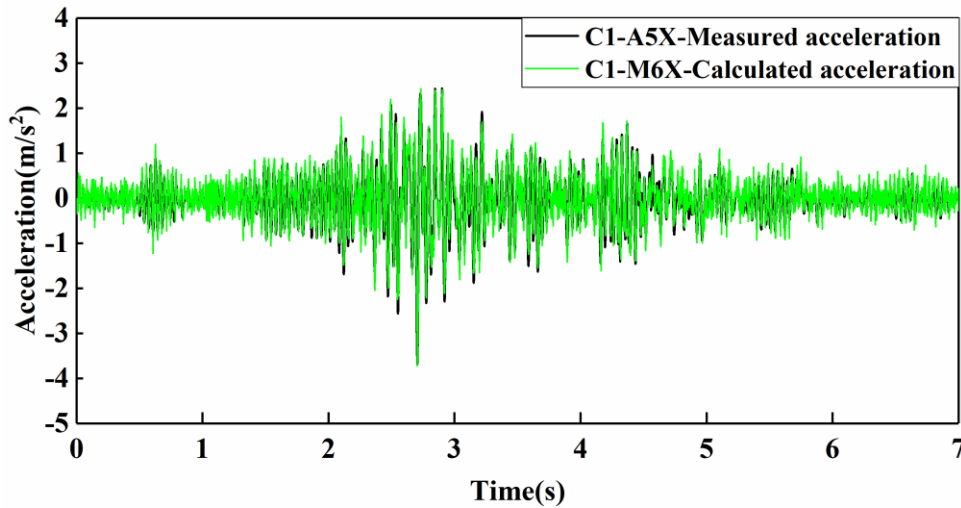


Fig. 6 – Time history of acceleration (C1-A5X-M6X)

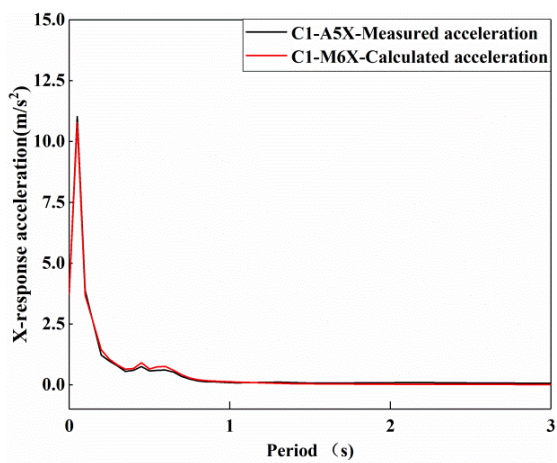


Fig. 7 – Response spectrum curve of acceleration (C1-A5X-M6X)

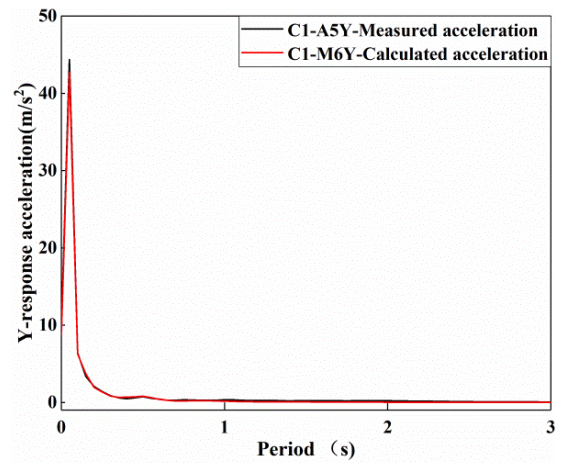


Fig. 8 - Response spectrum curve of acceleration (C1-A5Y-M6Y)



5.1.2 Case 2

The relative errors of the two kinds of absolute maximum acceleration under the excitation of case 2 are shown in Table 3. When the number of smoothing points is 7 to 11, the relative error of the maximum acceleration in the X direction is within 1.57% to 15.67%; the optimal smoothing point is 7 points, and the relative error is 1.57%. For calculated acceleration in the Y direction, the optimal number of smooth points is 9 points, the relative error is 9.75%, and the relative errors of the other smooth points are greater than 20%. Fig. 9 and Fig. 10 are the two response spectrum curves of acceleration in the X and Y directions, respectively. The two curves basically coincide, indicating that the two accelerations fit well.

Table 3 – C2-The relative error of maximum acceleration (M6-A5)

Direction	The number of points	The maximum measured acceleration (m/s ²)	The maximum calculated acceleration (m/s ²)	Relative error (%)
X	5	3.19	3.97	24.45
	7		3.24	1.57
	9		2.92	8.46
	11		2.69	15.67
	13		2.45	23.20
Y	5	8.51	17.22	102.35
	7		10.60	24.56
	9		7.68	9.75
	11		5.81	31.73
	13		4.98	41.48

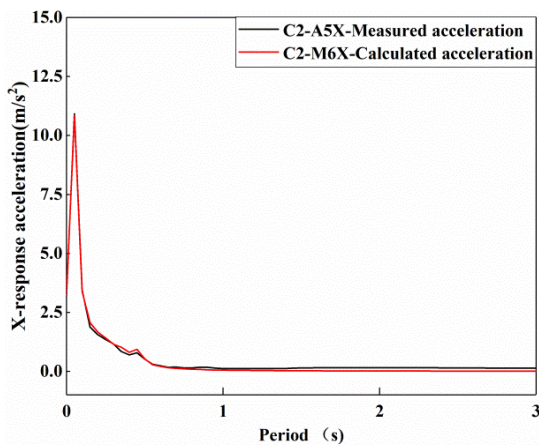


Fig. 9 - Response spectrum curve of acceleration (C2-A5X-M6X)

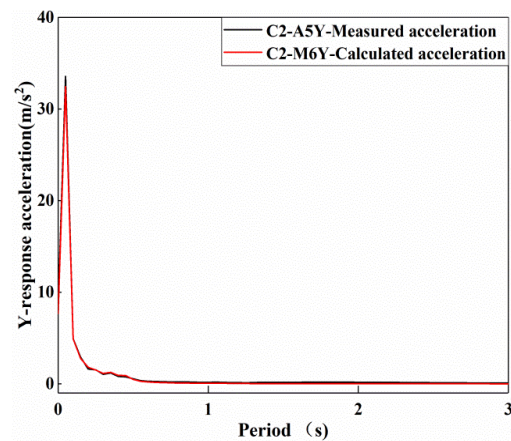


Fig. 10 – Response spectrum curve of acceleration (C2-A5Y-M6Y)

5.2 Results of M4

5.2.1 Case1

As shown in Table 4, for X direction acceleration, when the number of smooth points is 5 to 13 points, the relative error of maximum value is within 19%. The optimal smooth point is 9 points, and the corresponding relative error is 0.62%. When the number of smooth points is 7 points, the relative error is 9.94%. The relative error is within 17% when the number of smoothing points is 7 to 11 in the Y direction; the optimal smoothing number is 7 and the error is only 1.24%; when the number of smoothing points is 9, the relative error is 10.14%. Figs. 11 to 14 show the two types of response spectra of acceleration when the number of smooth points in the X and Y directions is 7, and 9, respectively. When the number of smooth points is 7



points, the response spectrum curves of the two directions basically coincide, and the fitting degree is good; when the number of smooth points is 9 points, the Y direction fits well, but the response spectrum of calculated acceleration in the X direction is smaller than the measured acceleration at the peak, the maximum difference between the two is 7.26% and the rest is basically coincident.

Table 4 – C1-The relative error of maximum acceleration (M4-A4)

Direction	The number of points	The maximum measured acceleration (m/s ²)	The maximum calculated acceleration (m/s ²)	Relative error (%)
X	5	4.83	5.73	18.63
	7		5.31	9.94
	9		4.80	0.62
	11		4.35	9.94
	13		3.99	17.39
Y	5	9.66	18.88	95.45
	7		9.54	1.24
	9		8.68	10.14
	11		8.08	16.36
	13		7.71	20.19

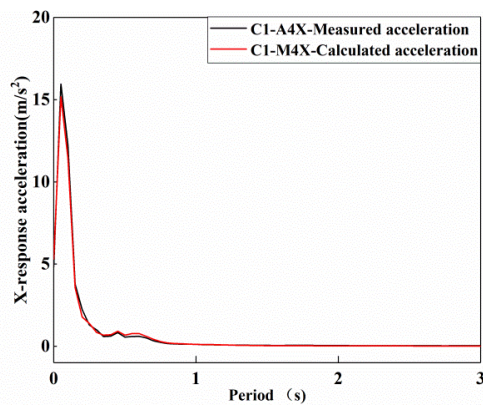


Fig. 11 – Response spectrum curve of acceleration (2-7-C1-A4X-M4X)

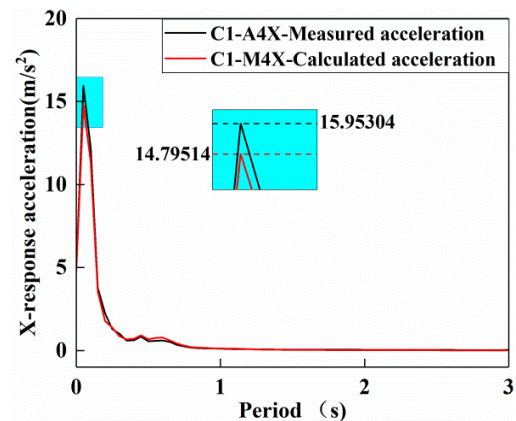


Fig. 12 – Response spectrum curve of acceleration (2-9-C1-A4X-M4X)

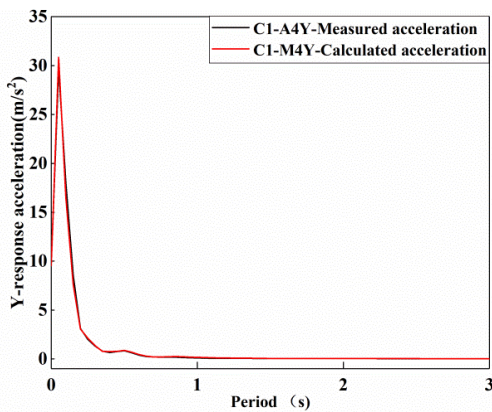


Fig. 13 – Response spectrum curve of acceleration (2-7-C1-A4Y-M4Y)

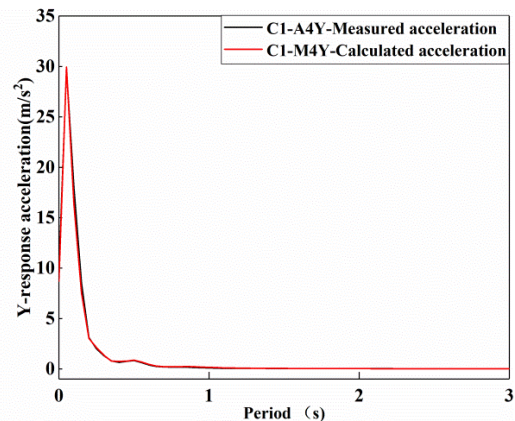


Fig. 14 – Response spectrum curve of acceleration (2-9-C1-A4Y-M4Y)



5.2.2 Case 2

As shown in Table 5, when the number of smoothing points is 7 or 9, the relative error of maximum value between the two types of accelerations in the X direction is within 10%. The optimal smoothing point is 7 points and the relative error is 3.36%. When the number of smooth points is 9 points in the Y direction, the relative error of maximum value is 13.43%. As shown in Figs. 15 and 16, and the fitting degrees in both directions are good.

Table 5 – C2-The relative error of maximum acceleration (M4-A4)

Direction	The number of points	The maximum measured acceleration (m/s ²)	The maximum calculated acceleration (m/s ²)	Relative error (%)
X	5	5.06	6.27	23.91
	7		5.23	3.36
	9		4.60	9.09
	11		4.02	20.55
	13		3.69	27.08
Y	5	9.31	20.63	121.59
	7		11.46	23.09
	9		8.06	13.43
	11		7.49	19.55
	13		6.92	25.67

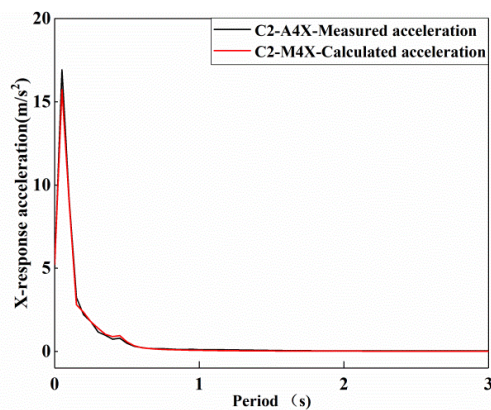


Fig. 15 – Response spectrum curve of acceleration (2-7-C2-A4X-M4X)

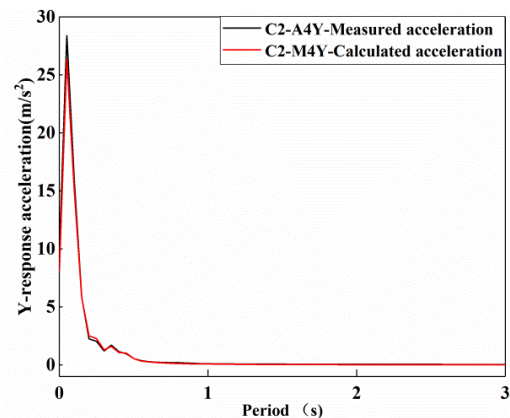


Fig. 16 – Response spectrum curve of acceleration (2-9-C2-A4Y-M4Y)

5.3 Result analysis of M2

5.3.1 Case 1

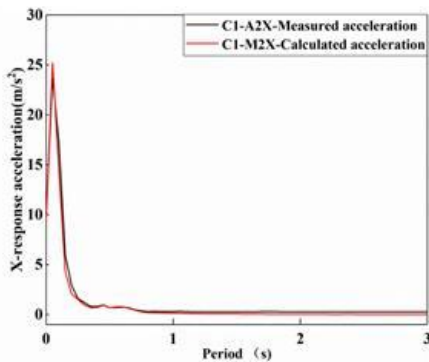
As shown in Table 6, for X direction acceleration, the error is less than 20% when the number of smooth points is 5 to 9; the optimal smooth point is 5 points and the relative error is 3.55%; when the number of smooth points is 7 points, the relative error is 11.27%. Fig. 17 is the response spectrum curves of acceleration when the number of smooth points is 5 and 7. The two curves basically coincide and fit well.



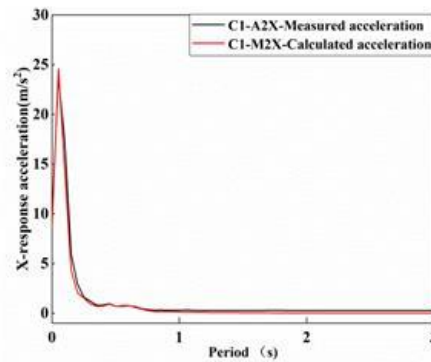
For Y direction acceleration, when the number of smooth points is 7 to 11, the relative errors of maximum acceleration are less than 12%, of which the optimal smooth point is 9 points, and the corresponding error is 3.13%; As shown in Fig. 18, the response spectrum of calculated acceleration is smaller than the response spectrum of measured acceleration near the peak. The maximum difference between the two is 11.7%. The rest of the curve basically coincides and the fit is fine.

Table 6 – C1-The relative error of maximum acceleration (M2-A2)

Direction	The number of points	The maximum measured acceleration (m/s ²)	The maximum calculated acceleration (m/s ²)	Relative error (%)
X	5	9.85	9.50	3.55
	7		8.74	11.27
	9		7.98	18.98
	11		6.93	29.64
	13		6.09	38.17
Y	5	18.56	22.69	22.25
	7		19.44	4.74
	9		19.14	3.13
	11		16.36	11.85
	13		14.55	21.61



(a) (2-5-C1-A2X-M2X)



(b) (2-7-C1-A2X-M2X)

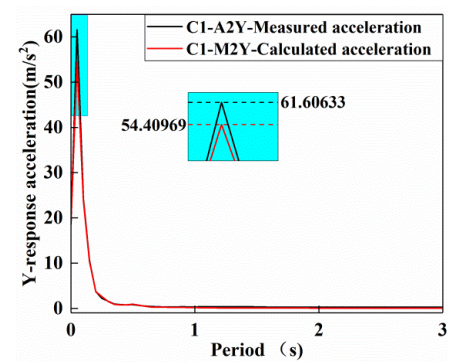


Fig. 18 – Response spectrum curve of acceleration (2-9-C1-A2Y-M2Y)

Fig. 17 – Response spectrum curve of acceleration.

5.3.2 Case 2

As shown in Table 7, for X direction acceleration, when the number of smooth points is 5 to 9, the relative error of maximum value is less than 15%. The optimal number of smoothing points is 7 points, and the relative error is 2.56%. Fig. 19 also shows that the two response spectrum curves of acceleration basically coincide and fits well.

For the Y direction acceleration, since the distance between the M2 and the A2 is far, when the number of smooth points is 7 points, the maximum relative error is 6.97%; the relative errors corresponding to the remaining points are all greater than 20%. Fig. 20 shows that the response spectrum of calculated acceleration is smaller than the response spectrum of measured acceleration near the peak. The maximum error between the two is 16.6%, and the degree of fitting is well.



Table 7 – C2-The relative error of maximum acceleration (M2-A2)

Direction	The number of points	The maximum measured acceleration (m/s ²)	The maximum calculated acceleration (m/s ²)	Relative error (%)
X	5	8.20	9.36	14.15
	7		7.99	2.56
	9		7.01	14.51
	11		6.39	22.07
	13		5.85	28.66
Y	5	15.36	23.54	53.26
	7		16.43	6.97
	9		12.19	20.64
	11		10.81	29.62
	13		9.72	36.72

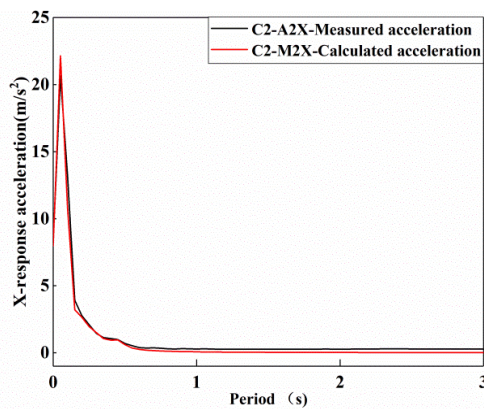


Fig. 19 – Response spectrum curve of acceleration (2-7-C2-A2X-M2X)

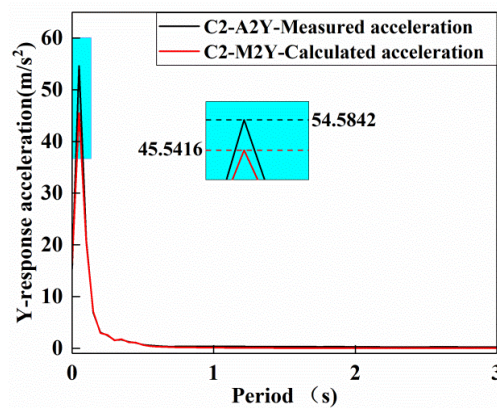


Fig. 20 – Response spectrum curve of acceleration (2-7-C2-A2Y-M2Y)

6. Conclusions

In this paper, the non-contact OC measurement technology was applied to the dynamic model tests of the hydraulic intake tower. The collected displacement data was subjected to S-G smooth filtering, and the acceleration was obtained through the second differential operation. The results show that the selection of smooth points in the S-G technology has a great influence on the validity of the calculated acceleration. The comparative analysis of the calculated and measured values of the accelerations of the three key positions at different elevations in the dynamic model test of the hydraulic intake tower under two sets of design-level earthquakes led to the following conclusion:

(1) There is a threshold for the number of smooth points. The closer this threshold is, the higher the accuracy of the calculated acceleration will be.

(2) For X-direction displacement data, when the smoothing points are odd points from 7 to 11, the minimum value of the relative error of the two accelerations can be as low as 0.54 %; the optimal smoothing point is 7 points, and the relative error is within 0.54% -11.27%. The two response spectrum curves of acceleration also basically coincide, and the fitting degree is very good.



(3) For the Y-direction displacement data, when the smoothing points are odd points from 7 to 11, the minimum value of relative error of maximum acceleration can as low as 1.24%. Considering the two aspects of the relative error of the maximum value and the fitting degree of the response spectrum, the optimal number of smooth points is 9 points, and the minimum value of the relative error can reach 3.13%.

In summary, after the displacement data was filtered and differentiated by the optimal smoothing parameter, the obtained acceleration data fits the measured acceleration data fairly well, which indicated the effectiveness and availability of using Optotrak-Certus to obtain acceleration data indirectly. The Optotrak-Certus non-contact technology combined with Savitzky-Golay smoothing technology can provide a new method with displacement and acceleration measurement of hydraulic structural dynamic model tests.

7. Acknowledgements

Special thanks are given to financial supports provided by the National Natural Science Foundation of China (No. 51709090), the Natural Science Foundation of Jiangsu Province (No. BK20170884), the Fundamental Research Funds for the Central Universities (No.2018B55714), and the Open Research Fund of State Key Laboratory of Simulation and Regulation of Water Cycle in River Basin (China Institute of Water Resources and Hydropower Research) (IWHR-SKL-KF201816).

8. References

- [1] Wang HB, Li DY, Chen HQ (2006): Experimental study on the dynamic failure of arch dams using a shaking table. *China Civil Engineering Journal*, 39(7), 109-118.
- [2] Wang HB, Li DY (2010): Experimental study of seismic overloading of large arch dam. *Earthquake Engineering & Structural Dynamics*, 35(2), 199-216.
- [3] Pan B, Xie H (2007): Full-Field Strain Measurement Based on Least-Square Fitting of Local Displacement for Digital Image Correlation Method. *Acta Optica Sinica*, CHINA, 27(11), 1980-1986.
- [4] Huang GP (2005): Research and Application of Key Technologies of Digital Close-up Industrial Photogrammetry. *Tianjin University*, CHINA.
- [5] M. Mynuddin Gani Mazumder, S. Kim, S.J. Park, Junsu Lee (2007): PRECISION AND REPEATABILITY ANALYSIS OF OPTOTRAK CERTUS AS A TOOL FOR GAIT ANALYSIS. *IFAC Proceedings Volumes*, 40(16), 107-112.
- [6] Goldsmith Jacob A, Trepeck Cameron, Halle Jessica L (2019): Validity of the Open Barbell and Tendo Weightlifting Analyzer Systems Versus the Optotrak Certus 3D Motion-Capture System for Barbell Velocity. *International Journal of Sports Physiology and Performance*, 14(4), 540-543.
- [7] Zhou Y (2017): Research on Performance Test Method of High Pile Wharf Based on DIC Measurement Technology. *Chongqing Jiao Tong University*, CHINA.
- [8] Xiao C (2014). Investigation of digital image correlation method in damage and fracture experiment. *Tianjin University*, CHINA.
- [9] Savitzky A, Golay M J E (1964): Smoothing and differentiation of data by simplified least squares procedures. *Analytical Chemistry*, 36(8), 1627-1639.
- [10] Zhou Z G, Tang P (2013): VI-Quality-Based Savitzky-Golay method for filtering time series data. *Remote Sensing Technology and Application*, CHINA, 28 (2) , 232-239.
- [11] Cai T, Tang H (2011): Overview of Least Square Fitting Principles of Savitzky- Golay Smoothing Filter. *Digital Communication*, CHINA, 38(01), 63-68.